A study on the characteristics of the marine boundary layer over Indian Ocean with ORV *Sagar Kanya* cruise # 120 during 1997

A. N. V. Satyanarayana, U. C. Mohanty* and N. V. Sam
Centre for Atmospheric Sciences, Indian Institute of Technology, New Delhi 110 016, India

The CLASS system observations of wind speed, wind direction, temperature and moisture at different pressure levels taken during the pre-INDOEX (Indian Ocean Experiment) cruise # 120 were used for the study. This article presents a study of marine boundary layer (MBL) characteristics, such as turbulent kinetic energy, MBL height, eddy diffusivity, etc. over the Indian Ocean using a multilevel one-dimensional PBL model with one and a half order TKE-ε closure scheme. The model also generates the vertical profiles of zonal wind, meridional wind, potential temperature and specific humidity. The model simulations are compared with the observations and the statistical analysis, viz. correlation coefficient; the RMS error is found to be satisfactory.

THE marine boundary layer (MBL) is in many ways quite different from that over land. The uniqueness is based on the fact that the liquid water is the lower boundary. MBL plays a pivotal role in the atmospheric energy studies. Comprehensive heat and moisture budget studies for the Atlantic Northeast and South East trade wind regime were made using data from 1925 through 1927 *Meteor* expedition. According to the data, there exists a net input of heat and moisture from the ocean into the atmosphere and the vertical structure of the MBL in the tropics and the subtropics depends on an interaction cycle of the air–sea energy and momentum exchange as well as the vertical transport mechanism and the large scale flow. As a result of the increased activity in numerical modelling, observational studies grew, particularly over the oceans at low latitudes. Some experiments such as International Indian Ocean Expedition (IIOE, 1963–65), Line Islands Experiment (LIE, 1967), Barbados Oceanographic Experiment (BOMEX, 1969), Atlantic Trade Wind Experiment (ATEX, 1969), Indo-Soviet Meteorological Expedition (ISMEX, 1973), GARP Atlantic Tropical Experiment (GATE, 1974), Air Mass Transformation Experiment (AMTEX, 1974–75) and Monsoon Experiment (MONEX, 1979) have provided data which include valuable information about the MBL.

Previous boundary layer research has been diverse. For instance, during IIOE, Bunker[1] had made a few boundary layer measurements. Ramanathan[2] assessed the bulk layer variations over the Arabian Sea along 10°N and along the equator, while Jambunathan and Ramamurty[3] focused on the sea and air temperature distributions over the Arabian Sea. Pant[4], on the other hand, discussed the vertical structure of the marine boundary layer in the West Indian Ocean, using the ISMEX data sets. Holt and Raman[5] studied the mean and turbulence structure of the monsoon MBL over the Bay of during MONEX-79.

Now INDOEX, a multi-agency, international field experiment scheduled for the winter monsoon of 1999, is one of first and major attempts to study the role that aerosols play in cooling the atmosphere, in the Inter-Tropical Convergence Zone (ITCZ) dynamics, MBL processes, etc. As a prelude to the main INDOEX, an intensive campaign during December 1996 to January 1997 has provided the necessary data sets for the present study. In this article, we examine the MBL characteristics such as MBL height, evolution of turbulent kinetic energy (TKE), and eddy diffusivity using a multi-level one-dimensional PBL model with TKE-ε closure scheme over Indian Ocean. The model also generated the vertical profiles of zonal and meridional wind, potential temperature and specific humidity.

Data

As a part of the pre-INDOEX research, upper air and surface observations have been taken over the Indian Ocean on-board ORV *Sagar Kanya* cruise # 120 from 27 December 1996 to 31 January 1997 (see Figure 1 of the Introductory Note). During this period, a total of 48 ascents of Vaisala radiosonde observations were taken at 6 h intervals. For the present study, three cases, i.e. 3–4 January 1997, 26–27 January 1997 and 29–30 January 1997 were chosen and include continuous data sets. A unique feature of the pre-INDOEX cruise # 120 was that the preferred CLASS sytem observation made the collection of vertical profiles of wind speed and wind direction, temperature and moisture at different pressure levels possible. Using a linear interpolation technique, the data sets

*For correspondence

of vertical profiles of above cited parameters were prepared at every 50 m in vertical from sea level to 2000 m depth column. These data sets were used as input in the PBL model to study the different characteristics of the MBL.

Model formulation

All computations presented here are performed with an one-dimensional TKE-ε closure scheme. The model has 40 levels in the vertical, with ΔZ as 50 m from the surface to 2000 m. An overview of the model is presented in Table 1.

Model equations

In the Descartes system of co-ordinates x, y and z, where the horizontal axes x and y are directed to the east and north respectively, and the vertical axis z is directed upward, the planetary boundary layer equations can be written in the following form[6,7]:

$$\frac{\partial u}{\partial t} = -\frac{\partial \overline{u'w'}}{\partial z} + fv - \tilde{p}_x/\tilde{\rho}, \tag{1}$$

$$\frac{\partial v}{\partial t} = -\frac{\partial \overline{v'w'}}{\partial z} - fu - \tilde{p}_y/\tilde{\rho}, \tag{2}$$

$$\frac{\partial \theta}{\partial t} + u\tilde{\theta}_x + \tilde{\theta}_y = -\frac{\partial \overline{\theta'w'}}{\partial z} + Q_r + Q_f, \tag{3}$$

Table 1. Overview of the model

Model description	1-D PBL model with one and half order TKE-ε closure scheme.
Vertical domain	Surface to 2000 m
Vertical levels	40, ΔZ = 50 m
Independent variables	Z, t
Prognostic variables	U, V, θ, q, q_w, E, ε
Diagnostic variables	K_u
Numerical scheme	Second order accuracy
Time integration	Implicit, Δt = 600 sec
Boundary conditions	For lower boundary, Monin–Obukhov similarity theory For upper boundary, the geostrophic conditions, actual observed values at 2000 m for TKE, ε, zero energy flux at 2000 m
Physical processes	Dry and moist convective adjustment Sensible and latent heat fluxes Fluxes under stormy conditions Longwave and shortwave radiation fluxes

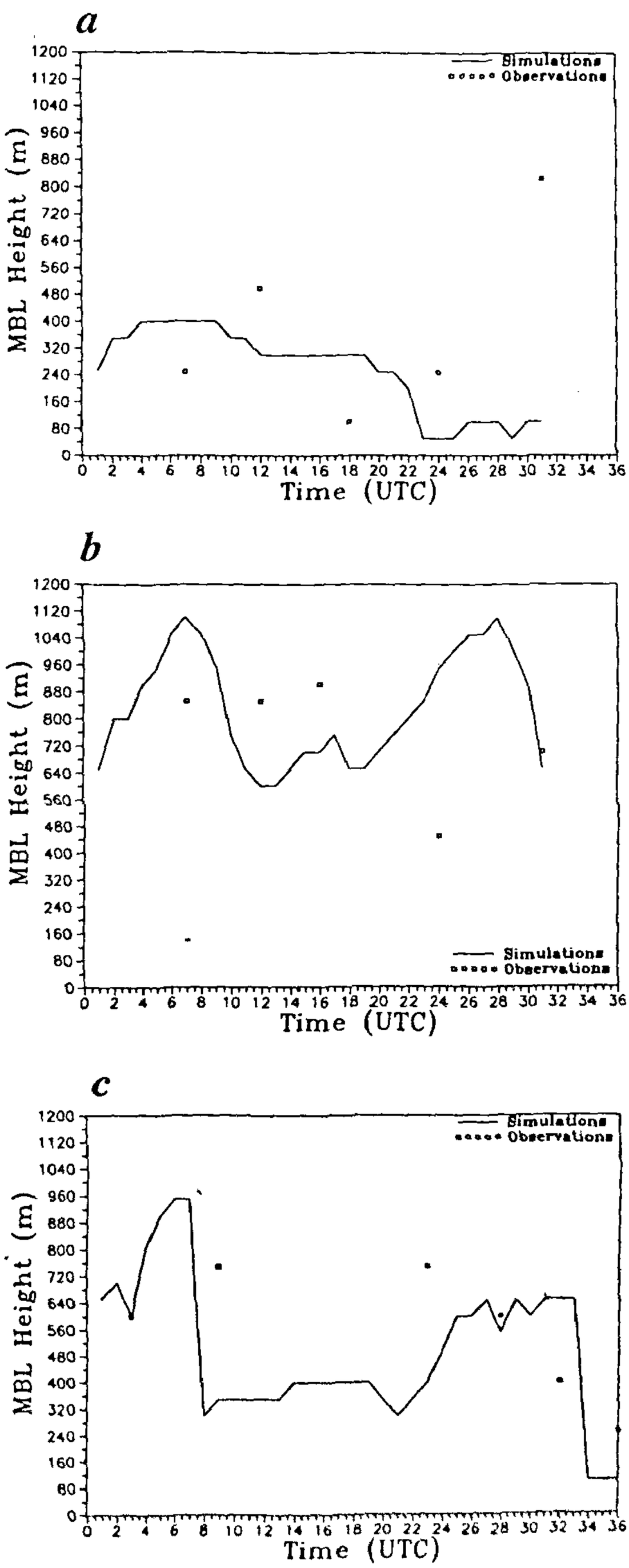

Figure 1. Diurnal variation of marine boundary layer height (m) during (*a*) 3–4 January 1997, (*b*) 26–27 January 1997 and (*c*) 29–30 January 1997.

$$\frac{\partial q}{\partial t}+u\tilde{q}_x+\tilde{q}_y=-\frac{\partial \overline{q'w'}}{\partial z}+E-C, \quad (4)$$

$$\frac{\partial q_w}{\partial t}+u\tilde{q}_{wx}+\tilde{q}_{wy}=-\frac{\partial \overline{q_w'w'}}{\partial z}-E+C-P, \quad (5)$$

$$\frac{\partial p}{\partial z}=-g\rho, \quad (6)$$

$$p=\rho RT, \quad \rho=\rho_a(1+0.61q-q_w), \quad (7)$$

$$\theta=T\left(\frac{p_o}{p}\right)^{\frac{R}{C_P}}, \quad (8)$$

where u, v, and w are x-, y- and z-components of the wind velocity, θ the potential temperature, T the absolute temperature, q the specific humidity, q_w the specific liquid-water content, p the pressure, ρ_a the density of dry air, ρ the density of the air–water–water vapour mixture (p_x, p_y), (σ_x, σ_y), (q_x, q_y) are components of horizontal gradients of the pressure, potential temperature, specific humidity and specific liquid–water content in the free atmosphere, Q_r and Q_f are rates of the heat change due to radiation and phase transitions of the water, C and E the rates of phase changes: water vapour to liquid water and water to water vapour, P the precipitation rate, $\rho\overline{u'w'}$, $\rho\overline{v'w'}$, $\rho\overline{\theta'w'}$, $\rho\overline{q'w'}$ and $\rho\overline{q_w'w'}$ the vertical turbulent fluxes of momentum, heat, water vapour and liquid water, R the universal gas constant, C_P the specific heat at constant pressure, p_o 1000 hPa, f the coriolis parameter and g the acceleration due to gravity.

Turbulent closure

In the model, the atmospheric boundary layer is partitioned into two sub-domains, one is near-surface constant flux layer ($z \le h$) and the other is free atmosphere topped interfacial layer ($h < z \le H$). It is assumed that h and H do not vary in time. In order to calculate vertical turbulent fluxes of momentum and heat and moisture in the interfacial layer, the Boussinesq hypothesis is used:

$$\overline{a'w'}=-K_a\frac{\partial a}{\partial z}, \quad (9)$$

where a is any of the prognostic variables u, v, θ, q and q_w, K_a the eddy exchange coefficient. It is assumed that $K_a=\alpha_a$, where α_a is dimensionless constant (equal to unity for the momentum flux). The coefficient of K is related to the turbulent kinetic energy E and the dissipation rate ε by the Kolmogorov[8] equation

$$K=\frac{C_k E^2}{\varepsilon}, \quad (10)$$

where C_k is a dimensionless constant. To compute E and ε, the following additional prognostic equations are used:

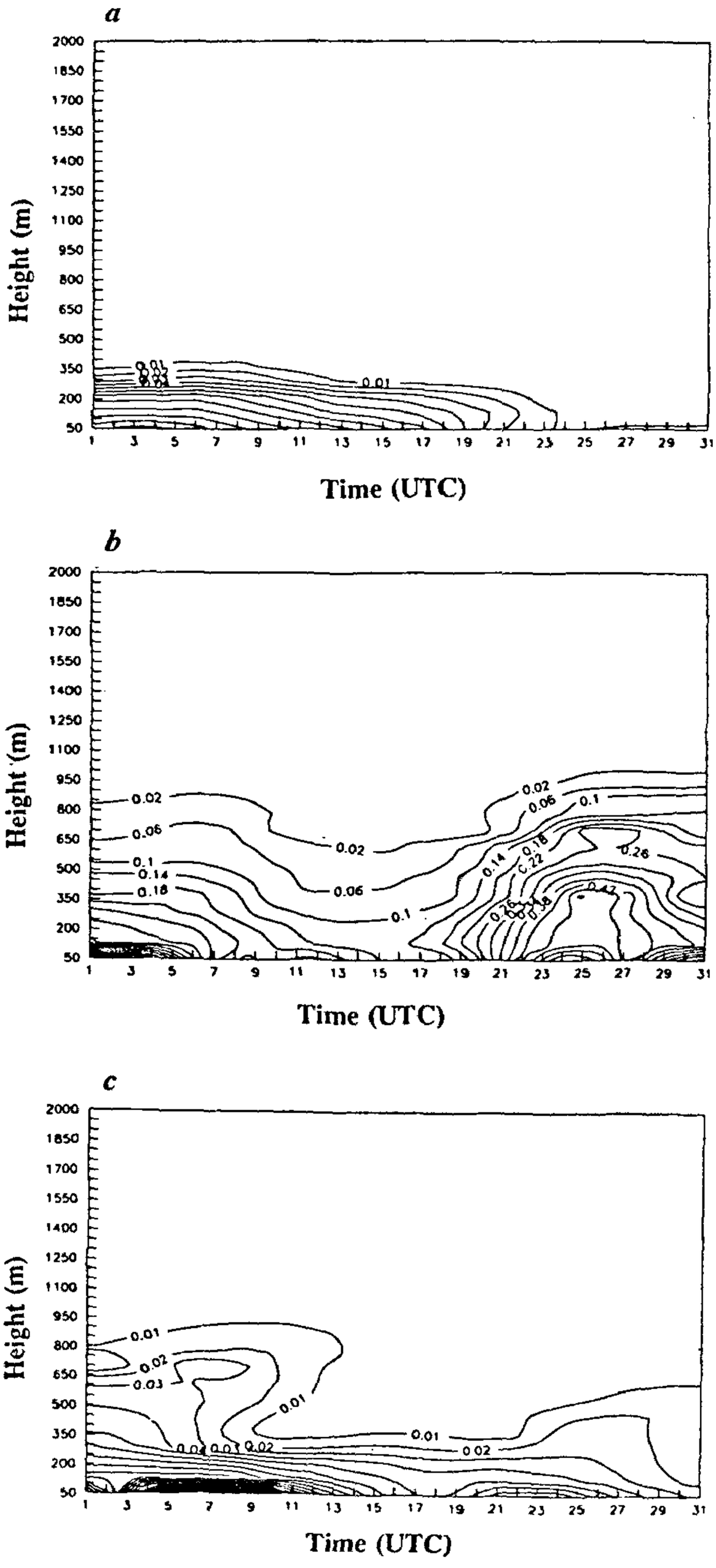

Figure 2. Time evolution of TKE ($m^2\ s^{-2}$) during (*a*) 3–4 January 1997, (*b*) 26–27 January 1997 and (*c*) 29–30 January 1997.

$$\frac{\partial E}{\partial t}=\left(-\overline{u'w'}\frac{\partial u}{\partial z}+\overline{v'w'}\frac{\partial v}{\partial z}+\frac{g}{\rho}\overline{\rho'w'}+\varepsilon\right)-\frac{\partial \overline{w'E'}}{\partial z}, \quad (11)$$

$$\frac{\partial \varepsilon}{\partial t}=-C_1\frac{\varepsilon}{b}\left(-\overline{u'w'}\frac{\partial u}{\partial z}+\overline{v'w'}\frac{\partial v}{\partial z}+\frac{g}{\rho}\overline{\rho'w'}+\varepsilon\right)-\frac{\partial \overline{w'\varepsilon'}}{\partial z}. \quad (12)$$

Here, the dimensionless parameters C_1 and b are computed as suggested by Aupoix *et al.*[9].

To compute the turbulent fluxes of TKE and dissipation rate, the down-gradient hypothesis is used:

$$\overline{w'E'}=-\alpha_E K\frac{\partial E}{\partial z}, \quad (13)$$

$$\overline{w'\varepsilon'}=-\alpha_\varepsilon K\frac{\partial E}{\partial z}, \quad (14)$$

where α_E and α_ε are dimensionless constants. We assumed that $\alpha_E=\alpha_\varepsilon=0.73$, and $\alpha_\theta=\alpha_q=\alpha_{qw}$, the value of α_θ is then calculated using the constant flux layer theory.

Lower boundary conditions

The lower boundary of the interfacial layer is kept as the maximum height of the constant flux layer. Then, the lower boundary conditions for the prognostic variables at the constant flux layer height, $z=h$, are as follows:

$$K\frac{\partial u}{\partial z}=C_D\left|\vec{V}_h\right|u_h, \quad (15)$$

$$K\frac{\partial v}{\partial z}=C_D\left|\vec{V}_h\right|v_h, \quad (16)$$

$$K_\theta\frac{\partial \theta}{\partial z}=C_\theta\left|\vec{V}_h\right|(\theta_h-\theta_s), \quad (17)$$

$$K_\theta\frac{\partial q}{\partial z}=C_\theta\left|\vec{V}_h\right|(q_h-q_s). \quad (18)$$

Here the subscript h indicates that the corresponding quantities refer to the upper boundary of the constant flux layer, whereas the subscript s refers to the quantities determined at the air–ocean interface. The drag (C_D) and heat exchange (C_θ) coefficients are calculated on the basis of Monin-Obukhov similarity theory.

The lower boundary conditions for the dissipation rate is

$$\varepsilon=\frac{u_*^3}{kh}[\phi_M(h/L)-h/L], \quad (19)$$

and for TKE is

$$\begin{aligned} E&=3.75u_*^2 && \text{for} \quad h/L\geq 0\\ &\left[3.75+(-h/L)^{3/2}\right]u_*^2+0.4w_*^2 && \text{for} \quad h/L\prec 0, \end{aligned} \quad (20)$$

where u_* the friction velocity, w_* the convective velocity scale and L the Monin-Obukhov length scale.

Upper boundary conditions

The maximum height of the turbulent boundary layer (top of the PBL) is chosen as the upper boundary. At the top of the boundary layer, the wind speeds, the potential temperature and the moisture attain the observed values at that height. The TKE flux and dissipation flux are assumed to vanish at that height. After analysing all the available data under consideration from the potential profiles, it is observed that the boundary layer height does not exceed 1500 m; therefore, the top of the model domain was kept at 2000 m.

Accordingly at $z=H$,

$$\bar{U}=U_H, \quad (21)$$

$$\bar{V}=V_H, \quad (22)$$

$$\bar{q}=q_H, \quad (23)$$

$$\bar{\theta}=\theta_H, \quad (24)$$

$$\frac{\partial \bar{e}}{\partial Z}=0, \quad (25)$$

$$\frac{\partial \bar{\varepsilon}}{\partial Z}=0. \quad (26)$$

The time variations of observations are obtained by the linear interpolation of the upper air measurements.

Initial conditions

For case 1, i.e. 3–4 January 1997, initial conditions were prepared using 01 UTC radiosonde observations and the model is integrated for 31 h.

For case 2, i.e. 26–27 January 1997, initial conditions were prepared using 00 UTC radiosonde observations and the model is integrated for 31 h.

For case 3, i.e. 29–30 January 1997, initial conditions were prepared using 03 UTC radiosonde observations, and the model is integrated for 36 h.

The time step of integration of the model was 600 sec, and hourly simulations of the model were stored for comparison with the observations.

Results and discussion

The results consist of the simulations of vertical profiles of zonal and meridional components of wind, potential temperature, specific humidity and eddy diffusivity; diurnal variation of marine boundary layer height; temporal variation of turbulent kinetic energy for all the cases as cited above. The model gives hourly simulations, but the simulations are compared with the available observations.

The observed profiles of zonal and meridional wind component, potential temperature and specific humidity obtained from CLASS measurements are linearly interpolated in the vertical and the obtained values at every 50 m interval up to 2000 m were used to compare with the simulations.

Marine boundary layer height

The model simulation of diurnal variation of MBLH for case 1, case 2 and case 3 is presented in Figure 1. The observed MBLH is also presented whenever available, and its variation is plotted with respect to simulation hours in UTC on the abscissa. For example, in Figure 1 *a*, 1st hour of simulation is read as 02 UTC of 3 January 1997, 25th hour as 02 UTC of 4 January 1997. Similarly in Figure 1 *b*, 1st hour of simulation as 02 UTC of 26 January 1997 and 25th hour as 02 UTC of 27 January 1997 and in Figure 1 *c*, 1st hour of simulation as 04 UTC of 29 January 1997 and 25th hour as 04 UTC of 30 January 97.

The observed MBLH is inferred from the potential temperature profiles of the radiosonde data. The height at which the potential temperature tends to increase was considered as the MBLH. In other words, the base of the stable layer has been taken as MBLH.

From the model simulations, very little diurnal variation of MBLH has been found in Figure 1 *a*. A maximum MBLH of 400 m has been observed, and a minimum MBLH of 80 m is simulated at around 23rd hour of simulation (00 UTC on 4 January 1997). Except at 08 UTC on the same date, the observations are reasonably matched.

Strong variations of MBLH appear in Figure 1 *b*. At the 1st hour of simulation (02 UTC, 26 January 1997) the simulated MBLH is 640 m, then reaches a maximum of 1100 m at the 8th hour before decreasing to a minimum of 600 m at 12th hour. A secondary peak of 740 m is simulated at 17th hour. Again a maximum of 1120 m is seen at 28th hour of simulation. The simulation of MBLH agrees reasonably well with the observations albeit with some difference in magnitude.

From Figure 1 *c*, no specific variation in the simulations of MBLH is noticed. A maximum MBLH of 960 m

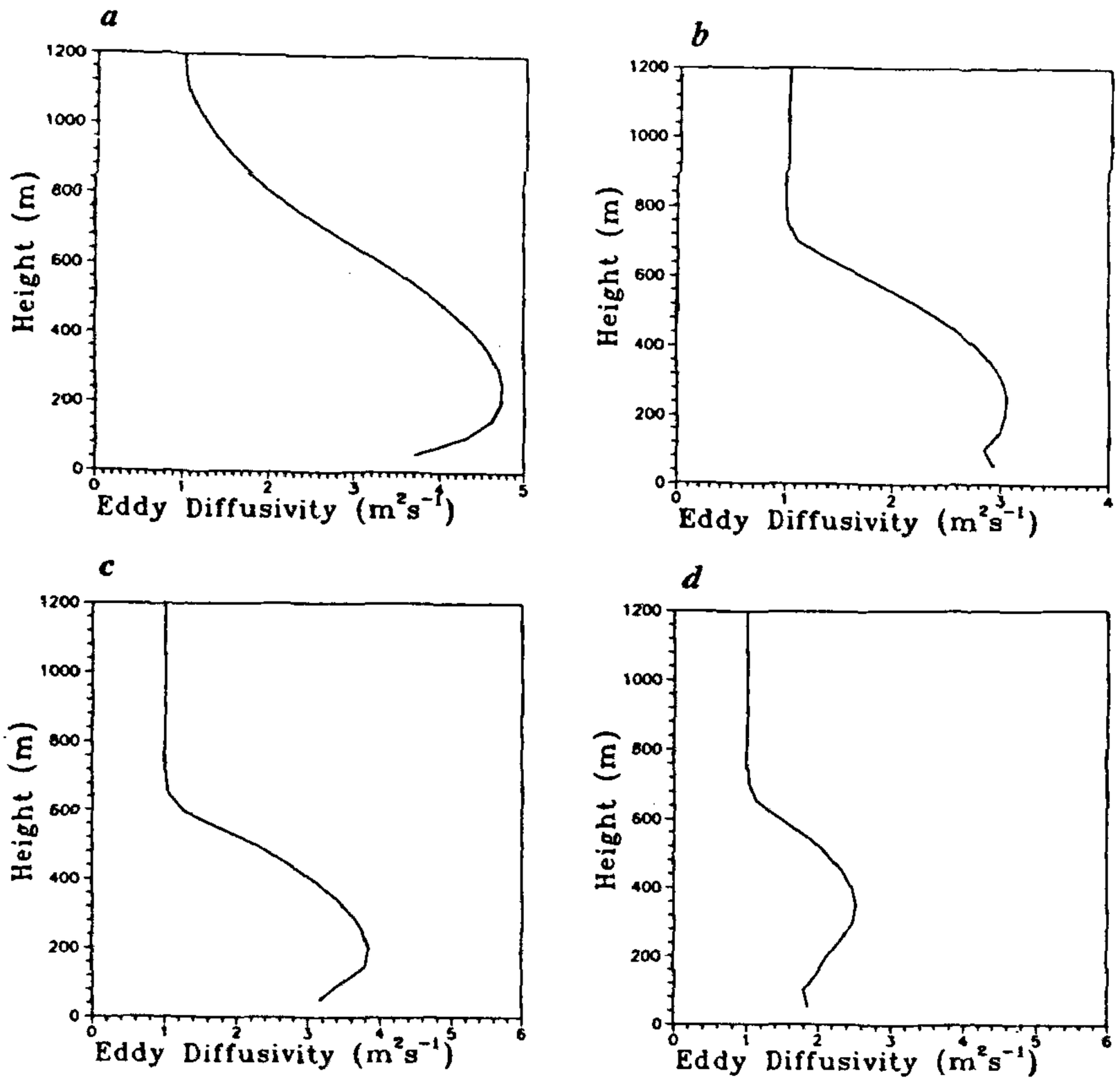

Figure 3. *a*, Vertical profile of eddy diffusivity ($m^2 s^{-1}$) at 09 UTC on 29 January 1997. *b*, same as (*a*) but for 16 UTC on 29 January 1997. *c*, same as (*a*) but for 04 UTC on 30 January 1997. *d*, same as (*a*) but for 05 UTC on 30 January 1997.

is simulated at the 3rd hour of simulation and drastically decreases to 300 m at 5th hour. In the aftermath not much variation is noticed up to 21st hour. Then it steadily increases to a maximum of 640 m at the 24th hour, and overall the model simulations reasonably agrees with the observed MBLH.

In general, during winter the boundary layer height over a desert region would go up to 1500 m in the mid-day and collapse in the evening hours to 50 m or so due low level inversion. However, over ocean, the boundary layer height would not vary much. In the present cases, usually the MBLH changes between 400 m and 1200 m, however, some strong variation occurs, which may be attributed to the presence of low level jets.

Evolution of turbulent kinetic energy

The model simulation of temporal variation of TKE for case 1, case 2 and case 3 is presented in Figure 2.

Not much variation in TKE is seen (Figure 2 *a*), and its intensity of TKE is low. It can be attributed to little mixing resulting in minimum MBLH as can be seen from Figure 1 *a*.

In contrast, a strong variation of TKE with time appears in Figure 2 *b*. Two distinct pockets of TKE variation with height and time, one between 1st and 13th hour of simulation and the other between 19th and 31st hour, are noticed. While second pocket exhibits more TKE variation than the first, both pockets signify the growth of the MBL.

TKE variation with height shifts to the 1st to 11th hour of simulation in Figure 2 *c*. Afterwards not much activity is visible until 21st hour of simulation, while later a few more TKE variations are seen. No specific diurnal variation of TKE is observed.

Overall the evolution of TKE reveals that much variation is visible except in case 2 and case 3, perhaps because of the mechanical generation of TKE with the presence of strong low level jets.

Eddy diffusivity profiles

A few simulated eddy diffusivity profiles are presented in Figure 3. In all these cases, the typical variation of eddy

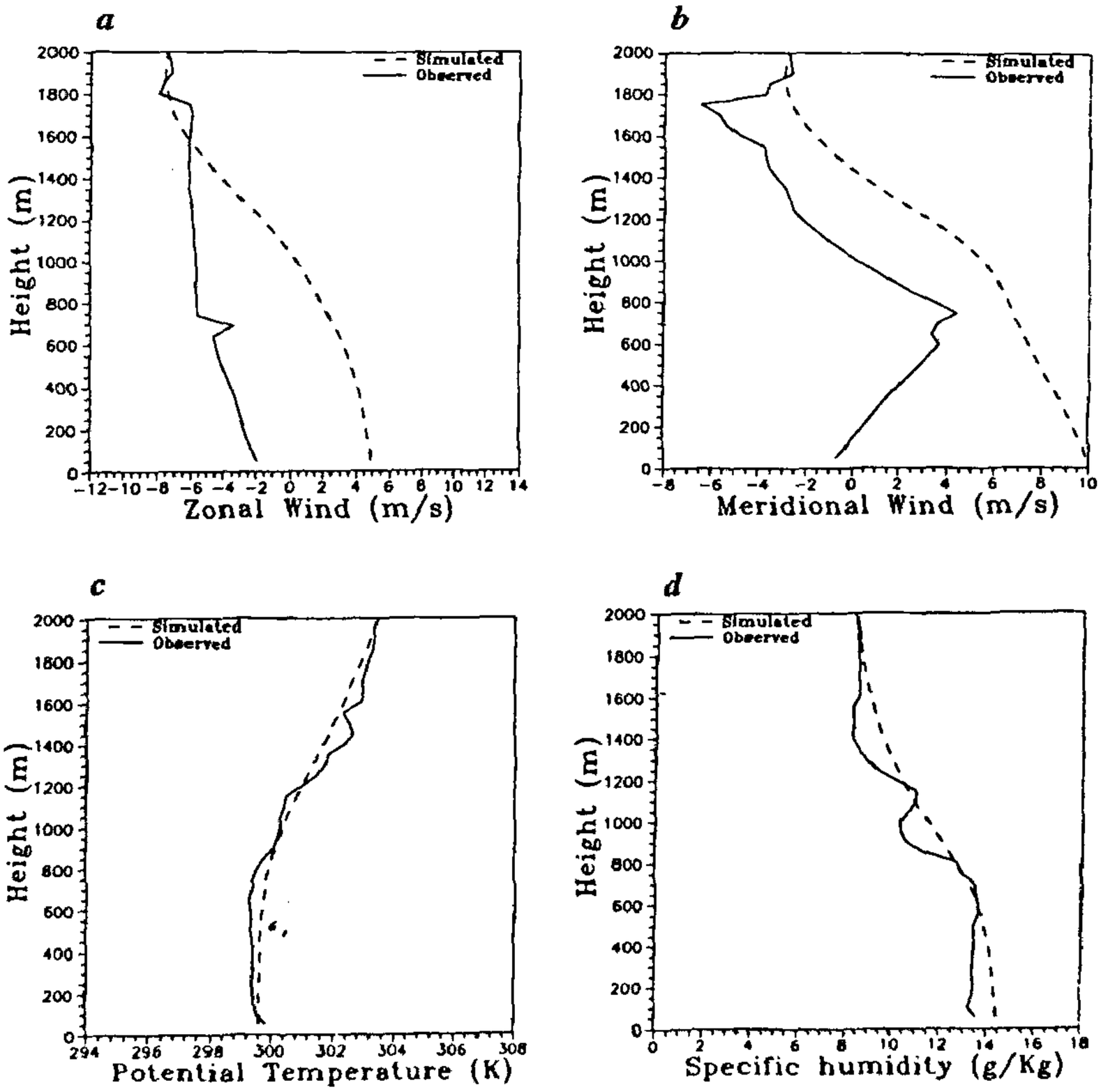

Figure 4. Vertical profiles of (*a*) zonal wind (m/s), (*b*) meridional wind (m/s), (*c*) potential temperature (*K*), and (*d*) specific humidity (g/kg) at 3rd hour of simulation (06 UTC on 29 January 1997).

diffusivity with height is noticed. In all the figures, there is an initial increase to a certain height and then a decreasing trend unfolds, which later becomes constant with height corroborating the typical eddy diffusivity profiles given in the literature.

Validation of the model

The model also generated the vertical profiles of zonal and meridional wind, potential temperature and specific humidity. In all the cases under consideration, the model simulations of zonal and meridional wind are comparatively reasonable with the observations with some deviations whereas potential temperature and specific humidity are in good agreement. The nature of variation of these basic meteorological fields is almost similar. As seen in Figures 4 and 5 respectively, the simulations at 3rd hour (06 UTC on 29 January 1997) and 28th hour (07 UTC on 30 January 1997) of these meteorological parameters along with the observations of one case i.e. case 3 are presented. The 3rd hour simulation of potential temperature agrees with the observations in the entire vertical column of 2000 m with a variation of less than 0.5 K. Similarly the 3rd hour simulation of specific humidity compares well with the observation with a maximum deviation of less than 1 g/kg. For the zonal winds, the 3rd hour simulation shows more deviation in the lower few hundred meters of the boundary layer with respect to observations; it then converges at the top of the model domain whereas in the case of meridional wind a large deviation of up to 500 m and an almost constant deviation in the higher layers occur.

The 28th hour simulation of potential temperature reveals a deviation of 2 K up to 600 m and less than 1 K in the higher layers with respect to observations. A maximum deviation of 4 g/kg is noticed between 600 m and 1400 m layer in the 28th hour of simulation of specific humidity. There is a deviation of the simulated zonal wind profile from the observed profile up to a height of 1200 m, while the simulated profile of the meridional wind posseses a similar orientation, but the deviation is greater than that of the zonal wind.

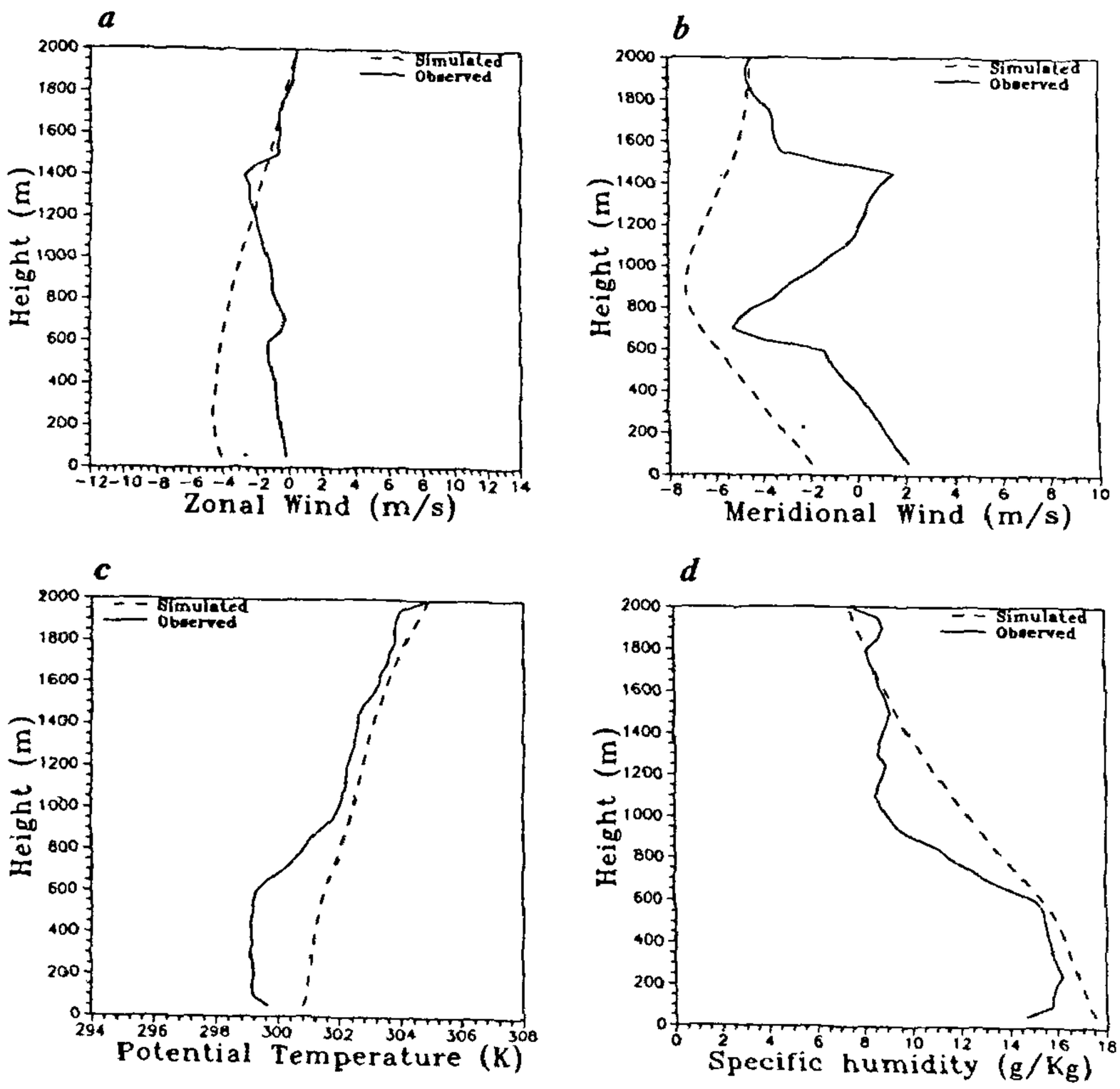

Figure 5. Vertical profiles of (*a*) zonal wind (m/s), (*b*) meridional wind (m/s), (*c*) potential temperature (*K*), and (*d*) specific humidity (g/kg) at 28th hour of simulation (07 UTC on 30 January 1997).

Table 2. Statistical evaluation of the performance of the model in the simulation of zonal wind (m/s), meridional wind (m/s), potential temperature (K) and specific humidity (g/kg)

Simulation hours for case 1/case 2/ case 3	Parameter	Case-1		Case-2		Case-3	
		RMS error	Corr. coeff.	RMS error	Corr. coeff.	RMS error	Corr. coeff.
7/7/9	U	1.00	0.51	5.28	0.82	7.51	0.60
	V	1.04	0.43	2.22	0.81	0.95	0.95
	θ	0.27	0.99	0.82	0.98	2.64	0.92
	q	0.71	0.98	2.73	0.94	5.35	0.78
24/24/23	U	0.77	0.74	3.53	0.60	0.50	0.90
	V	1.44	0.25	2.72	0.29	4.26	0.30
	θ	0.00	0.99	2.97	0.93	0.00	0.96
	q	2.26	0.83	3.19	0.96	0.96	0.98
31/31/32	U	2.09	0.47	2.66	0.78	2.92	-0.29
	V	1.30	0.87	1.01	0.89	1.68	0.87
	θ	0.74	0.95	0.35	0.96	0.89	0.81
	q	0.42	0.97	3.86	0.78	2.51	0.85

Statistical analysis

The correlation coefficient and root mean square (RMS) error of the model in the simulations of zonal and meridional wind, potential temperature and specific humidity at different simulation hours for all the three cases are presented in Table 2. Barring a few, in all the three cases at all the simulations hours the simulations of zonal and meridional wind, potential temperature and specific humidity are well correlated with the observations. The RMS error of these parameters is comparatively less in case 1 than in case 2 and case 3. The RMS error of the potential temperature in all the cases is reasonably small and specific humidity follows next. Though in permissible limits, the RMS errors of the zonal and meridional wind in particular are relatively more in case 2 than in others.

Conclusions

The results for three simulation cases lead to the following broad conclusions:

(i) The MBLH over the relatively homogeneous ocean surfaces does not show much diurnal variation. The MBLH variation during the period of study is confined between 400 m and 1120 m. Any occasional variation of MBLH is mainly due to the presence of strong low level winds with occurrence of low level jet.

(ii) The generation of TKE is normally due to either mechanical forcing or thermal production, and its evolution shows no specific temporal variation. Due to the presence of strong winds the mechanical forcing induced TKE variation is noticed in some cases. In such cases the magnitude of the TKE is found to be 0.44 $m^2 s^{-2}$, one order more than in calm wind conditions.

(iii) The vertical distribution of eddy diffusivity in the marine boundary layer increases in the first few hundred meters with a maximum value of 5 $m^2 s^{-1}$ almost 300 m and then decreases. The nature of the variation of eddy diffusivity agrees well with other studies.

(iv) The model simulation of vertical profiles of potential temperature and specific humidity also agreed well with the observations. The model simulations of zonal and meridional wind agree reasonably with the observations and deviations are noticed with increase in time of integration. This can be attributed to local variations and advection processes, which are not considered in 1-D models.

(v) Finally, in conformation with these results, the RMS error is found to be less than expected in potential temperature and specific humidity simulations. In case of zonal and meridional wind, the RMS error is reasonable. The model simulations of potential temperature and specific humidity are highly correlated with observations.

1. Bunker, A., Proc. Symp. IIOE, Bombay, 1965, pp. 3–16.
2. Ramanathan, Y., *Indian J. Meteorol. Hydrol. Geophys.*, 1978, **29**, 643–654.
3. Jambunathan, R. and Ramamurthy, K., *Indian J. Metorol. Geophys.*, 1975, **25**, 377–410.
4. Pant, M. C., *Indian J. Meteorol. Hydrol. Geophys.*, 1978, **29**, 88.
5. Holt, T. and Sethu Raman, *Mon. Wea. Rev.*, 1986, **114**, 2176–2190.
6. Lykossov, V. N. and Platov, G. A., *Russ. J. Numer. Anal. Math. Modeling*, 1992, **7**, 419–440.
7. Kusuma, G. Rao, Lykossov, V. N., Prabhu, A., Sridhar, S. and Tonkacheyev, E., *Proc. Indian Acad. Sci. (Earth Planet. Sci.)*, 1996, **105**, 227–260.
8. Kolmogorov, A. N., *Izv. Akad. Nauk SSSR Ser. Fiz.*, 1942, **6**, 56–58.
9. Aupoix, B., Cousteau, J. and Liandrat, J., *Turbulent Shear Flows*, 1986, **6**, 6–17.

ACKNOWLEDGEMENTS. We thank to Prof. Sethuraman, NCSU, Raleigh, USA, Prof. V.N. Lykossov, INM, Russia and Prof. A. P. Mitra, Chairman, INDOEX-India programme, for encouragement and needful scientific discussions. This work was partly supported by INDOEX, Indian component, CSIR, DST, Govt of India and ONR, USA.